Human Molecular Genetics, 2021, Vol. 30, No. 7 564–574

doi: 10.1093/hmg/ddab071
Advance Access Publication Date: 11 March 2021
General Article

GENERAL ARTICLE

Humanization of a tandem repeat in IG-DMR causes stochastic restoration of paternal imprinting at mouse *Dlk1-Dio3* domain

Satoshi Hara[1,2], Miho Terao[1], Atsumi Tsuji-Hosokawa[1], Yuya Ogawa[1,3] and Shuji Takada[1,3,*]

[1]Department of Systems BioMedicine, National Research Institute for Child Health and Development, Tokyo 157-8535, Japan, [2]Division of Molecular Genetics & Epigenetics, Department of Biomolecular Science, Faculty of Medicine, Saga University, Saga 849-8501, Japan and [3]Department of NCCHD, Graduate School of Medical and Dental Sciences, Tokyo Medical and Dental University (TMDU), Tokyo 113-8510, Japan

*To whom correspondence should be addressed at: Department of Systems BioMedicine, National Research Institute for Child Health and Development, 2-10-1 Okura, Setagaya, Tokyo 157-8535, Japan. Tel/Fax: +81-3-3417-2498; Email: takada-s@ncchd.go.jp

Abstract

The *Dlk1-Dio3* imprinted domain, regulated by an intergenic differentially methylated region (IG-DMR), is important for mammalian embryonic development. Although previous studies have reported that DNA methylation of a tandem repeated array sequence in paternal IG-DMR (IG-DMR-Rep) plays an essential role in the maintenance of DNA methylation in mice, the function of a tandem repeated array sequence in human IG-DMR (hRep) is unknown. Here, we generated mice with a human tandem repeated sequence, which replaced the mouse IG-DMR-Rep. Mice that transmitted the humanized allele paternally exhibited variable methylation status at the IG-DMR and were stochastically rescued from the lethality of IG-DMR-Rep deficiency, suggesting that hRep plays a role in human IG-DMR for the regulation of imprinted expression. Moreover, chromatin immunoprecipitation analysis showed that TRIM28 was enriched in hypermethylated paternal hRep without ZFP57. Our results suggest that hRep contributes to the maintenance of human IG-DMR methylation imprints via the recruitment of TRIM28.

Introduction

Genomic imprinting is an epigenetic phenomenon involving parental-origin-specific expression of genes, termed imprinted genes. Imprinted genes tend to form imprinting clusters, and are regulated by imprinting control regions (ICRs) acting in *cis* (1). Most ICRs are 'marked' by paternal- or maternal-specific epigenetic modifications such as DNA methylation; these regions are referred to as differentially methylated regions (DMRs). It is known that there are two types of DMRs: germline and somatic. While the majority of DNA methylation established during gametogenesis is erased after fertilization, sperm- or oocyte-specific DNA methylation involving germline DMRs is protected from active/passive demethylation and is maintained throughout embryogenesis and adulthood. On the

Received: February 9, 2021. **Revised:** February 9, 2021. **Accepted:** March 4, 2021

© The Author(s) 2021. Published by Oxford University Press.
This is an Open Access article distributed under the terms of the Creative Commons Attribution Non-Commercial License (http://creativecommons.org/licenses/by-nc/4.0/), which permits non-commercial re-use, distribution, and reproduction in any medium, provided the original work is properly cited. For commercial re-use, please contact journals.permissions@oup.com

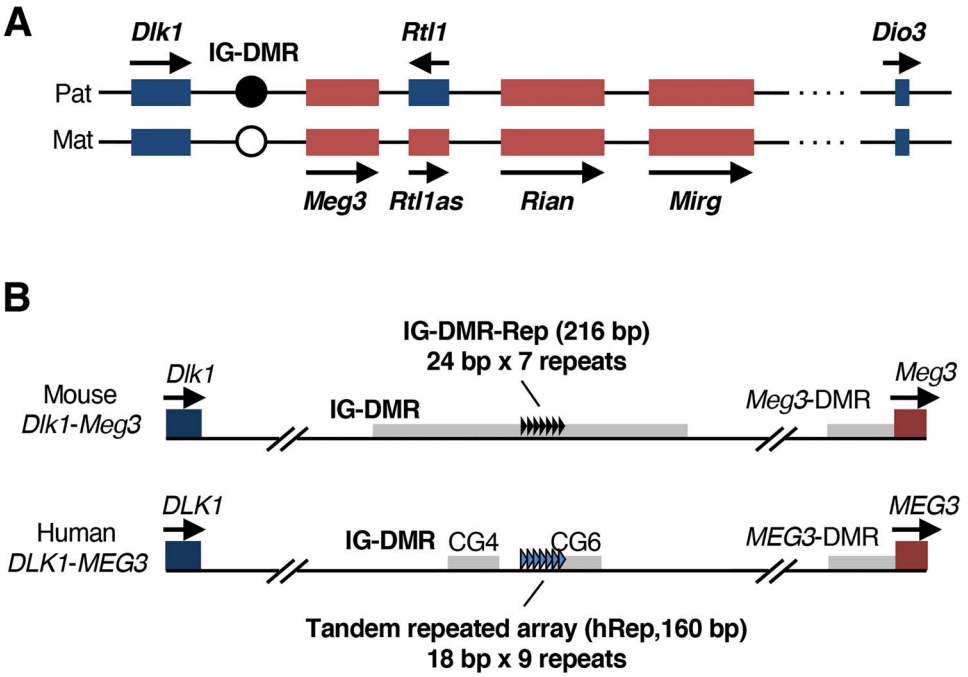

Figure 1. Mouse and human *Dlk1-Dio3* domain. (**A**) Schematic representation of mouse *Dlk1-Dio3* domain. Genomic DNA is indicated by a black line. Imprinted genes expressed from paternal and maternal alleles are shown in blue and red boxes, respectively. Arrows indicate direction of transcription and expressed alleles. Methylated and unmethylated IG-DMRs are shown in a black and a white circle, respectively. (**B**) Schematic representation of mouse and human *Dlk1-Meg3* region. IG-DMR (note that human IG-DMR is divided into CG4 and CG6) and *Meg3/MEG3*-DMR are shown in gray boxes. Each repeat unit of IG-DMR-Rep and hRep is indicated by black and blue triangles, respectively.

other hand, allele-specific DNA methylation at somatic DMRs is only established during post-implantation development (2). Loss of DNA methylation involving either germline or somatic DMRs causes imprinting diseases due to aberrant expression of imprinted genes, indicating that maintenance of allele-specific DNA methylation at DMRs is essential for embryonic development.

One example of an imprinting cluster is the *Dlk1-Dio3* imprinted domain located on mouse chromosome 12/human chromosome 14, which is essential for embryonic development, encoding paternally expressed protein-coding genes (*Dlk1*, *Rtl1* and *Dio3*), and maternally expressed non-coding RNAs (*Meg3*, *Rtl1as*, *Rian* and *Mirg*) (3–9). Allele-specific expression of these imprinted genes at this locus is regulated by *Dlk1-Meg3* intergenic DMR (IG-DMR, germline DMR) and the promoter region of *Meg3* (*Meg3*-DMR, somatic DMR), which are specifically methylated on the paternal allele (Fig. 1A) (10). In humans, it is known that paternal and maternal uniparental disomy for chromosome 14, or large deletions including IG-DMR, cause imprinting disorders called Kagami-Ogata syndrome (KOS) and Temple syndrome (TS) (11,12). In particular, the phenotypes of KOS and TS patients resemble mice with uniparental disomy for chromosome 12, or mutated IG-DMR, suggesting that regulatory mechanisms involving IG-DMR are conserved between humans and mice (13–15). Although the molecular mechanisms of IG-DMR for imprinted expression of *Dlk1-Dio3* domain genes are well studied in mice, such molecular details surrounding human IG-DMR in the regulation of the *DLK1-DIO3* domain are still largely unclear.

Previously, we reported that a tandem repeated array sequence in IG-DMR (IG-DMR-Rep) is essential for the maintenance of DNA methylation imprints at the paternal IG-DMR (15,16). Mice lacking IG-DMR-Rep revealed that paternal transmission of the IG-DMR-Rep deletion allele results in loss of methylation imprints at paternal IG-DMR and embryonic lethality. Therefore, IG-DMR-Rep plays an essential role in the maintenance of paternal methylation imprint at IG-DMR. In mice, the key regulator of IG-DMR is ZFP57, the Krüppel-associated box (KRAB)-containing zinc finger protein (KRAB-ZFP), because it has been reported that maternal/zygotic knockout (KO) of *Zfp57* results in loss of IG-DMR methylation imprints (17). In fact, IG-DMR-Rep contains five putative ZFP57-binding motifs. It is known that ZFP57 interacts with its transcriptional cofactor, TRIM28 (also known as KAP1). TRIM28 confers DNA methylation and repressive histone marks (trimethylation of H3 Lys9; H3K9me3) to surrounding sequences by recruiting DNA methyltransferase DNMT1 and histone methyltransferase SETDB1 (18,19). In addition, recent studies have demonstrated that ZFP57 and TRIM28 are strongly enriched in IG-DMR-Rep by chromatin immunoprecipitation-sequencing (ChIP-seq) analysis of mouse embryonic stem cells (20,21). Taken together, these results suggest that IG-DMR-Rep functions as a scaffold for the ZFP57–TRIM28 complex to maintain the imprinting status of paternal IG-DMR. On the other hand, in humans, it has been reported that there are nine 18 bp units in the 160 bp CpG-rich region at IG-DMR (Fig. 1B and Supplementary Material, Fig. S1) (22). However, the function of this tandem repeated array sequence in human IG-DMR (referred to as hRep) is unknown. The difficulty of the functional analysis of hRep is that the sequence of tandem repeated arrays is not highly conserved between humans and mice, and there is no suitable animal model.

In this study, to clarify the molecular function of the hRep sequence in the human *DLK1-DIO3* domain, we generated model mice with hRep, which replaced endogenous murine IG-DMR-Rep.

Results

Generation of a mouse model by replacing IG-DMR-Rep with hRep

To understand the molecular mechanisms involved in IG-DMR-mediated imprinted gene expression in the *DLK1-DIO3* domain, we generated a murine model that replaced mouse IG-DMR-Rep with hRep using the CRISPR/Cas9 system. To this end, a single-guide RNA (sgRNA) and a targeting vector, consisting of hRep with 1 kb of mouse IG-DMR-Rep flanking sequence as homology arms, was designed. sgRNA/Cas9 and the targeting vector were injected into mouse zygotes, and three founder pups carrying the replaced allele were obtained (Fig. 2A). Of the three founders, only one female mouse transmitted the replaced allele to the next generation, whereas the other two mice were infertile (Supplementary Material, Fig. S2A). We note that the replaced allele of hRep contained a 1 nt substitution (G > A) that did not alter any CpG site in the original hRep sequence (Supplementary Material, Fig. S2B). Because fertile founder mice carrying a complete hRep sequence was never obtained from 630 injected and transferred embryos, we used the mouse line IG-DMR^{hRep} for subsequent experiments.

Paternal inheritance of the humanized allele stochastically restores embryonic lethality by IG-DMR-Rep deletion

Next, we crossed IG-DMR^{hRep} mice with wild-type C57BL/6 N (B6) mice to examine whether paternal or maternal transmission of the hRep allele has any effect on development and growth. The results showed that pups carrying the maternally inherited hRep allele were born in a Mendelian ratio and were indistinguishable from wild type (WT) mice, indicating that maternal transmission of hRep allele does not affect embryonic lethality. On the other hand, when B6 female mice were crossed with IG-DMR^{hRep} males, the average number of pups was lower (mean ± SD; 5.2 ± 2.4) than that of IG-DMR^{hRep} females crossed with B6 males (mean ± SD; 7.8 ± 1.9, $P < 0.01$, Student's *t*-test). In particular, the number of offspring carrying the hRep allele was significantly decreased, whereas the number of WT pups was not (Fig. 2B). These results implied that paternal transmission of the hRep allele results in embryonic lethality. Of the living pups with paternally transmitted hRep allele, some offspring exhibited significantly decreased body weight compared with that of WT mice and died within 24 h after birth (Fig. 2C). The remaining surviving pups showed similar body weight as that of WT animals, and grew normally to adulthood, indicating that paternal inheritance of the hRep allele, which does not contain ZFP57 binding motifs, rescued the offspring from the embryonic lethality observed in embryos with the paternal transmission of the IG-DMR-Rep deletion (Fig. 2C and D).

Because the survival rate of pups carrying paternally transmitted IG-DMR^{hRep} (IG-DMR$^{+/hRep}$) was lower than that in maternal transmission (IG-DMR$^{hRep/+}$), we next elucidated the phenotypes of IG-DMR$^{+/hRep}$ embryos at the mid-to-late gestation stage. At 14.5 days *post coitum* (dpc), all IG-DMR$^{+/hRep}$ embryos were alive and indistinguishable from WT. The fetal weights at this stage were similar to that of WT mice. On the other hand, the phenotypes of IG-DMR$^{+/hRep}$ embryos varied at 16.5 dpc (Fig. 3A). Among the IG-DMR$^{+/hRep}$ embryos, 11% (8 of 75) of embryos were indistinguishable from WT (grouped as 'rescued,' relative fetal weight: ≥0.9), whereas 17% (13 of 75) embryos exhibited growth retardation (grouped as 'growth retarded,' and relative fetal weight < 0.9). The other IG-DMR$^{+/hRep}$ embryos (22 of 75) were already dead at this stage (Fig. 3B and C), suggesting that the time of embryonic lethality occurred between 14.5 and 16.5 dpc. Taken together, these results indicated that paternal transmission of the hRep allele causes variable phenotypes during embryogenesis, and stochastically rescues a proportion of IG-DMR$^{+/hRep}$ embryos from perinatal lethality.

To elucidate the paternal hRep allele effect in placental development, placental phenotypes in IG-DMR$^{+/hRep}$ mice were analyzed. The results showed that the mean placental weights of IG-DMR$^{+/hRep}$ were significantly reduced at 14.5 and 16.5 dpc (Fig. 3D). Histological analysis of IG-DMR$^{+/hRep}$ embryos at 16.5 dpc revealed thinner labyrinth layers in growth-retarded IG-DMR$^{+/hRep}$ placentas, whereas no placental defects were observed in the rescued IG-DMR$^{+/hRep}$ (Supplementary Material, Fig. S3). These results suggested that the placentas were defective in IG-DMR$^{+/hRep}$ embryos, similar to IG-DMR$^{+/\Delta Rep}$, which had already commenced from 14.5 dpc.

Taken together, our results indicated that replacement of paternal IG-DMR-Rep with hRep causes variable growth retardation, whereas some IG-DMR$^{+/hRep}$ embryos could avoid the embryonic lethality caused by IG-DMR-Rep deficiency.

Imprinting status of Dlk1-Dio3 domain in IG-DMR$^{+/hRep}$ embryos

To elucidate the imprinting status of the humanized paternal allele and its effects on the imprinted region, we carried out DNA methylation analyses of IG-DMR and *Meg3*-DMR in IG-DMR$^{+/hRep}$ mice. Bisulfite sequencing analysis of IG-DMR, including endogenous IG-DMR-Rep and hRep, showed that the paternal hRep sequence was completely methylated, whereas endogenous IG-DMR-Rep at the maternal allele was completely hypomethylated in living IG-DMR$^{+/hRep}$ pups. In IG-DMR$^{hRep/+}$ pups, the maternally transmitted hRep sequence was hypomethylated, suggesting that the hRep sequence was subjected to paternal-specific methylation imprint (Supplementary Material, Fig. S4A and B). In addition, DNA methylation at *Meg3*-DMR was similar in surviving IG-DMR$^{+/hRep}$ and IG-DMR$^{hRep/+}$ pups (Supplementary Material, Fig. S4C). To determine whether there was a difference in methylation levels between living and dead individuals, we compared the methylation levels in each IG-DMR$^{+/hRep}$ offspring. The results showed that dead IG-DMR$^{+/hRep}$ pups presented a slight decrease in hRep methylation levels compared with those of living pups (alive vs. dead = 99% vs. 84%, $P = 0.05$; Supplementary Material, Fig. S4A). In the dead IG-DMR$^{+/hRep}$ pups, complete hypomethylation at *Meg3*-DMR was observed (Supplementary Material, Fig. S4C). These results suggested that incomplete imprinting of IG-DMR causes loss of methylation at the *Meg3*-DMR.

Next, we analyzed the DNA methylation status during embryonic development. Interestingly, bisulfite sequencing analysis of IG-DMR$^{+/hRep}$ embryos at 16.5 dpc showed that, on paternal hRep, DNA of individual embryos was methylated at various levels, ranging from 20% to 99% (Fig. 4A and Supplementary Material, Fig. S5A). Methylation levels at *Meg3*-DMR also varied, ranging from 4% to 50% in IG-DMR$^{+/hRep}$ individuals, the levels of which were positively correlated to those of hRep in each individual (Supplementary Material, Fig. S5B). To identify when the variation in DNA methylation levels at hRep occurred, we analyzed DNA methylation levels in individual IG-DMR$^{+/hRep}$ embryos at various embryonic stages. As a result, paternal hRep was found to be completely methylated in IG-DMR^{hRep} sperm; however, the various methylation statuses at paternal hRep were observed

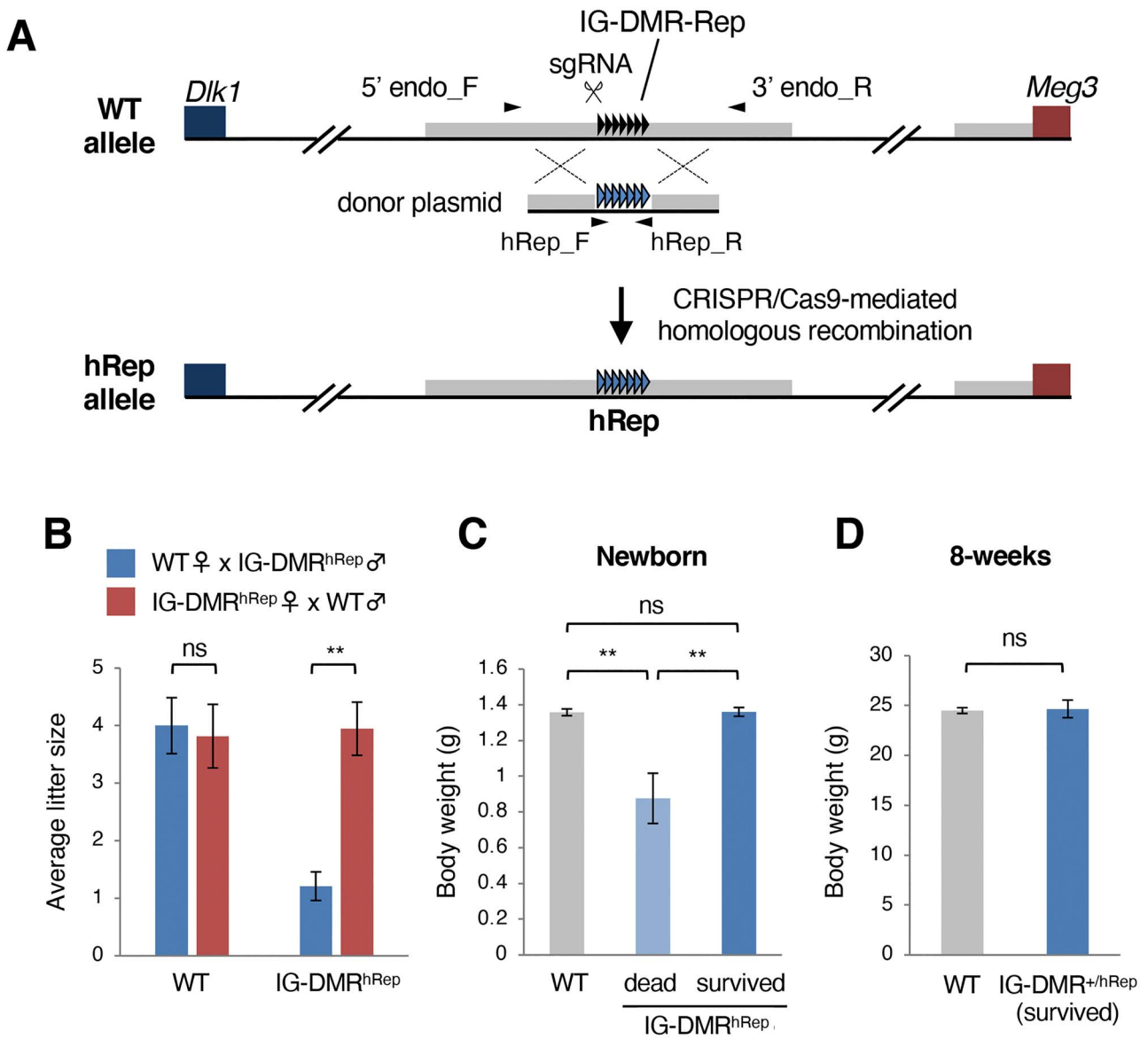

Figure 2. Generation of IG-DMR^{hRep} mice. (**A**) Schematic representation of generation of IG-DMR^{hRep} allele. Genomic DNA, genes, IG-DMR-Rep and hRep are indicated as for Fig. 1B. Primers for genotyping are shown by arrowheads. (**B**) Average litter sizes of pups inherited hRep allele from father and mother. Bar graph showing average number of WT and IG-DMR^{hRep} pups. Paternal ($n = 19$) and maternal ($n = 11$) transmission of hRep allele shown in blue and red, respectively. (**C**) Body weight of newborn pups. WT ($n = 40$), dead ($n = 3$) and surviving ($n = 8$) IG-DMR$^{+/hRep}$ are shown. (**D**) Body weight of 8-week-old WT ($n = 4$) and surviving IG-DMR$^{+/hRep}$ male mice ($n = 3$) are shown. The error bar shows standard error. $^{**}P < 0.01$. ns: not significant (Student's *t*-test).

at all stages of, and after, the blastocyst stage, suggesting that DNA methylation at hRep is stochastically lost during preimplantation development (Fig. 4B and Supplementary Material, Figs S6–S8).

To examine relationships involving the methylation status of paternal hRep and the expression of imprinted genes, we assessed expression levels in individual IG-DMR$^{+/hRep}$ embryos at 16.5 dpc. Quantitative RT-qPCR analysis showed that expression levels of *Dlk1* were reduced in individuals with hRep methylation levels less than 70% compared with those of WT mice, whereas embryos with hRep methylation levels more than 70% were the same as those of WT (Fig. 4C). This tendency was also observed in other paternally expressed genes, *Rtl1* and *Dio3* (Supplementary Material, Fig. S9). In contrast, the maternally expressed gene, *Meg3*, was overexpressed (1.5- to 2-fold) in individual IG-DMR$^{+/hRep}$ embryos, with less than 80% of hRep methylation levels, whereas *Meg3* expression levels were comparable with those of WT in IG-DMR$^{+/hRep}$ embryos with more than 80% hRep methylation (Fig. 4D).

To elucidate the influence of substitution of hRep in the surrounding IG-DMR region on DNA methylation, we analyzed the methylation status in two regions located upstream and downstream of IG-DMR-Rep (IG-DMR_R1 and IG-DMR_R2, respectively; Fig. 5A). To distinguish parental alleles by SNP genotyping, IG-DMR$^{+/hRep}$ embryos were generated by crossing IG-DMR^{hRep} male mice with JF1 females. The results showed that, on paternal hRep, 2 out of 9 embryos were completely methylated, whereas the remainder were methylated at <70% (Fig. 5B and Supplementary Material, Fig. S8A). On the other hand, paternal IG-DMR_R1 was methylated at >75% in most

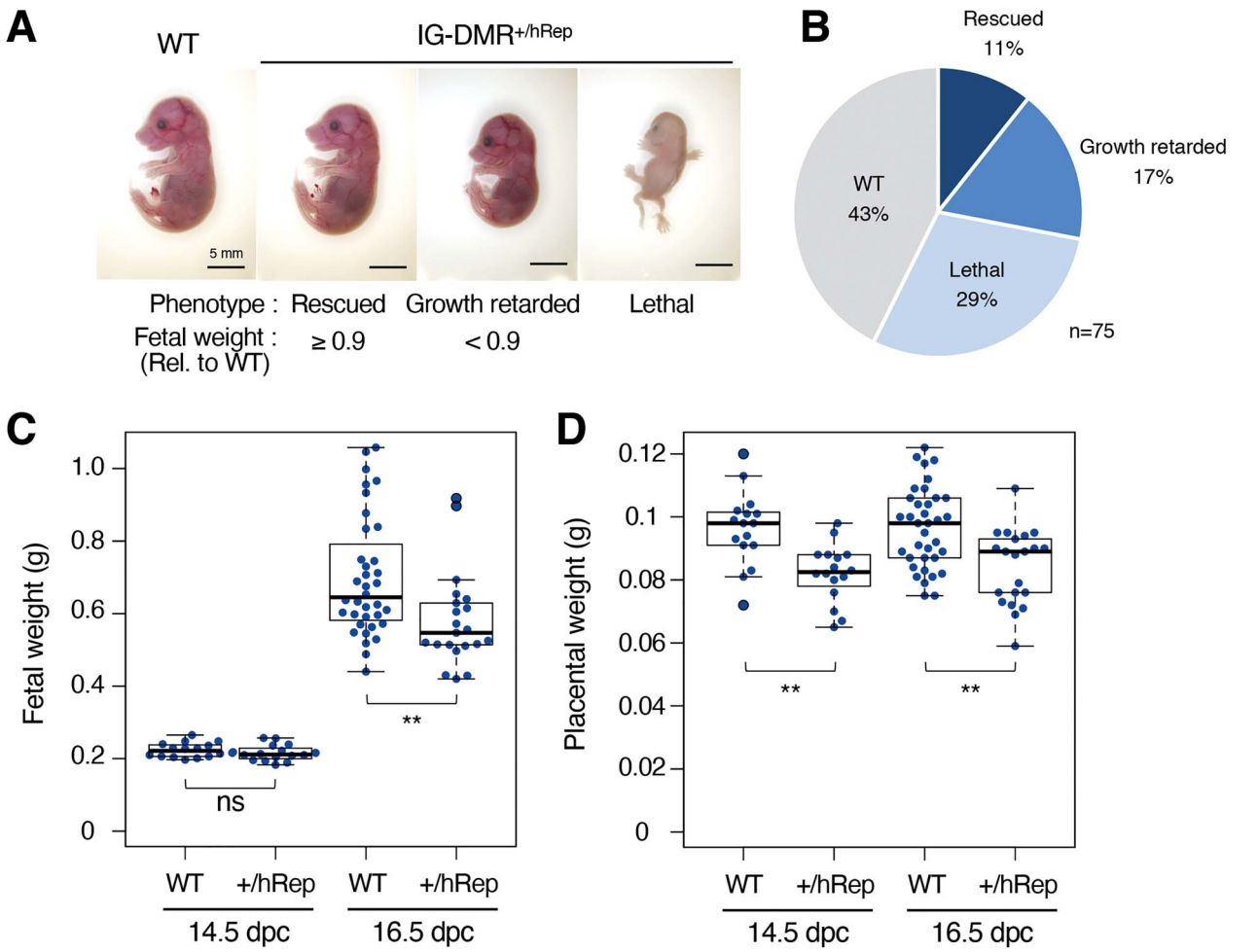

Figure 3. Phenotypes of IG-DMR$^{+/hRep}$ embryos. (**A**) Representative photograph of IG-DMR$^{+/hRep}$ embryos at 16.5 dpc. Each phenotype and relative fetal weight are shown under the image. (**B**) The proportion of numbers of mice with phenotypes in IG-DMR$^{+/hRep}$ embryos. 'WT' indicates littermate wild-type embryos. (**C, D**) Fetal body (C) and placental (D) weights of WT and IG-DMR$^{+/hRep}$ embryos at 14.5 and 16.5 dpc. Genotypes and stages are shown at the bottom. Beeswarm and boxplot indicates individual and statistical fetal weights, respectively. **; $P < 0.01$ (Student's *t*-test), ns; not significant.

IG-DMR$^{+/hRep}$ embryos (8 of 9), despite the hypomethylation of paternal hRep. In contrast, methylation analysis of paternal IG-DMR_R2 showed that this region was hypomethylated in 6 of 9 IG-DMR$^{+/hRep}$ embryos, whereas it was methylated by >80% in two embryos with completely methylated paternal hRep (Fig. 5C and Supplementary Material, Fig. S8B). These results suggested that incomplete hRep methylation is associated with methylation status in other regions of IG-DMR.

To test whether the methylation status of hRep influences the allelic expression of the imprinted genes, we analyzed the allelic expression of maternally expressed *Meg3* in IG-DMR$^{+/hRep}$ embryos. The results showed that parental origin-specific monoallelic expression of *Meg3* was observed in 2 embryos with completely methylated hRep, whereas *Meg3* was biallelically expressed in 6 of 9 embryos (Fig. 5D and Supplementary Material, Fig. S10). These results indicated that methylated hRep can function as an ICR in IG-DMR$^{+/hRep}$ embryos.

Taken together, our results indicated that variation in DNA methylation at the hRep sequence causes aberrant expression of imprinted genes, and leads to stochastic lethality (or survival) in IG-DMR$^{+/hRep}$ embryos.

TRIM28-dependent but ZFP57-independent maintenance of paternal imprinting in hRep embryos

It is known that the trimethylation of histone H3K9 mediated by the ZFP57–TRIM28 complex is essential for maintaining DNA methylation imprints at IG-DMR. To test whether H3K9me3 and ZFP57–TRIM28 complexes accumulate at the hRep sequence on the paternal allele, ChIP-qPCR analysis around the hRep sequence was carried out. Chromatin samples of WT, IG-DMR$^{hRep/+}$ and IG-DMR$^{+/hRep}$ embryos at 11.5 dpc were immunoprecipitated using antibodies against H3K9me3, ZFP57 and TRIM28. IG-DMR$^{+/hRep}$ embryos were classified into two groups by DNA methylation levels at the paternal hRep allele: methylated ≥ 90% and methylated < 90% (Supplementary Material, Fig. S7). To distinguish IG-DMR-Rep and hRep, we designed PCR primer sets to amplify only one of them (Fig. 6A). ChIP-qPCR analysis using primer set P1, which amplifies endogenous IG-DMR-Rep, showed that H3K9me3, ZFP57 and TRIM28 accumulated to high levels in paternal IG-DMR-Rep in IG-DMR$^{hRep/+}$ embryos, whereas no enrichment was observed for the maternal allele of IG-DMR$^{+/hRep}$ embryos (Fig. 6B). These results confirmed that the H3K9me3 and

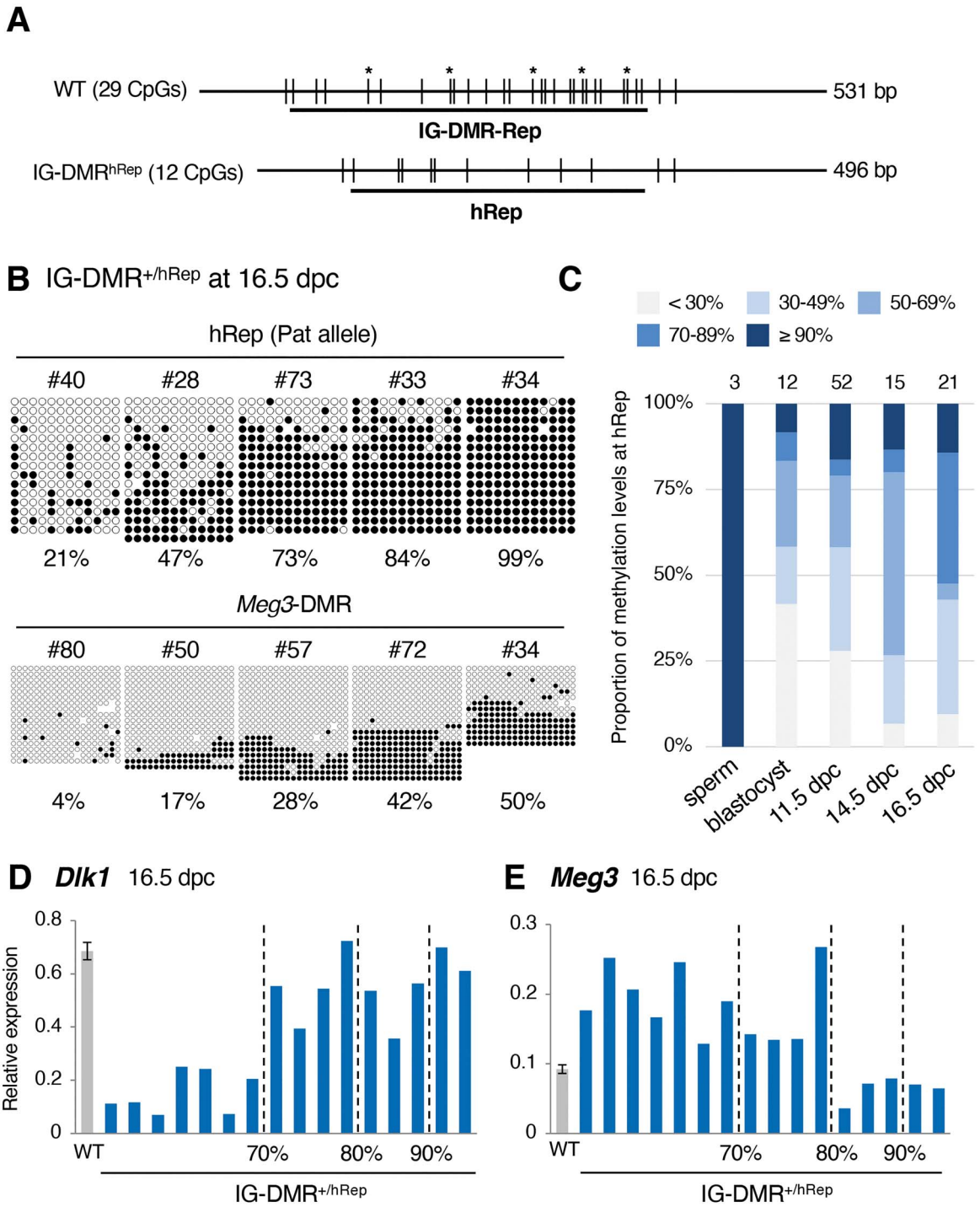

Figure 4. DNA methylation at hRep and expression of imprinted genes in IG-DMR$^{+/hRep}$ embryos. (**A**) Positions of CpG sites in the PCR product containing IG-DMR-Rep/hRep. Product sizes amplified from WT and IG-DMR^{hRep} alleles are indicated at the right. Vertical lines indicate the position of each CpG site. Asterisks indicate the CpG sites on ZFP57 binding motifs (TGCCGC). Positions of IG-DMR-Rep and hRep are shown as bold lines. (**B**) Representative methylation status of paternal hRep and *Meg3*-DMR in individual IG-DMR$^{+/hRep}$ embryos at 16.5 dpc. Methylated and unmethylated CpGs are shown in closed and open circles, respectively. Each number above the methylation status indicates individual sample ID. Percentages show methylation levels. (**C**) The proportion of embryos categorized by methylation levels at paternal hRep. Each fraction (<30%, 30–49%, 50–69%, 70–89% and ≥90%) is shown with colors indicated at the top. Numbers of examined embryos are shown above the bars. Full results of methylation status in individual embryos are shown in Supplementary Material, Figs S5–S8. (**D** and **E**) Expression levels of *Dlk1* (D) and *Meg3* (E) in individual IG-DMR$^{+/hRep}$ embryos at 16.5 dpc ($n = 16$ from 4 litters). Individual expression levels are sorted by methylation levels of paternal hRep. Gray bar indicates the average expression levels in WT ($n = 15$ from 4 litters).

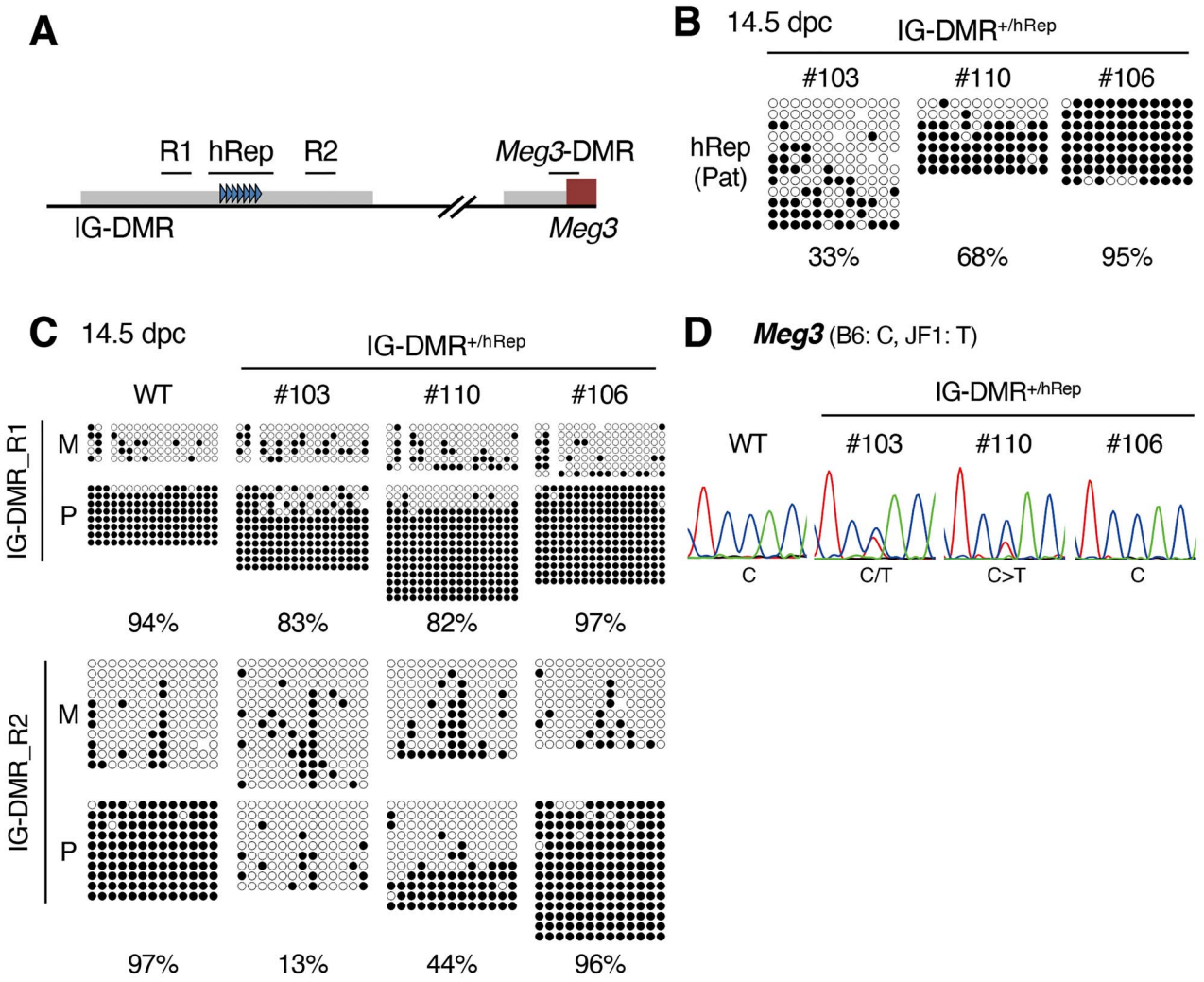

Figure 5. DNA methylation status at the region surrounding hRep. (**A**) Schematic representation of analyzed regions in IG-DMR. Genomic DNA, genes and hRep are indicated as for Fig. 2A. Amplified regions are indicated by black lines above IG-DMR. (**B**, **C**) Methylation status at paternal hRep (B), IG-DMR_R1 and IG-DMR_R2 (C) in IG-DMR$^{+/hRep}$ embryos at 14.5 dpc. Three representative embryos are shown. 'M' and 'P' indicates maternal and paternal alleles, respectively. Percentages indicate methylation levels of paternal alleles. (**D**) Allelic expression of *Meg3* gene in IG-DMR$^{+/hRep}$ embryos at 14.5 dpc. Electropherograms of PCR products amplified from three representative embryos are shown.

ZFP57–TRIM28 complex specifically accumulates at IG-DMR-Rep on the paternal allele.

Next, ChIP-qPCR analysis using hRep-specific primer set P2 revealed considerable enrichment of H3K9me3 at paternal hRep observed in the ≥90% methylated group, whereas moderate H3K9me3 levels were detected in the <90% methylated group. TRIM28 was also enriched in the ≥90% methylated group, while little TRIM28 accumulation was observed in the <90% methylated cohort. Because hRep contains no ZFP57 binding motifs, we assumed that ZFP57 was not enriched at paternal hRep. As expected, the enrichment levels of ZFP57 were similar between IG-DMR$^{hRep/+}$ and the <90% methylated group. However, only minor enrichment was observed in the ≥90% methylated group (Fig. 6C).

Since data obtained by ChIP-qPCR experiments tend to be affected by closely located DNA binding sequences, we elucidated the effects of the ZFP57 binding sequence next to the centromeric side of IG-DMR-Rep (IG-DMR_R1 region in Fig. 6A). To this end, ChIP-qPCR was performed to measure enrichment levels of H3K9me3, TRIM28 and ZFP57 using primer set P3 for IG-DMR_R1. The results showed that the enrichment levels of ZFP57 in the <90% methylated and ≥90% methylated groups were lower than those of IG-DMR$^{hRep/+}$, suggesting that enrichment levels observed for hRep (P2 primer set) were not affected by the ZFP57 binding sequence present on IG-DMR_R1. As for TRIM28, the enrichment levels among IG-DMR$^{hRep/+}$, <90% methylated group, and ≥90% methylated group were not correlated between experiments using P2 and P3. This situation was also applicable to H3K9me3 enrichment (Fig. 6D).

Taken together, our results indicated that the ≥90% methylated group, hRep, was able to recruit TRIM28 and establish repressive IG-DMR histone marks, independent of ZFP57-mediated DNA binding.

Discussion

We generated humanized mice by replacing IG-DMR-Rep with a tandem repeat array sequence from humans. Since the

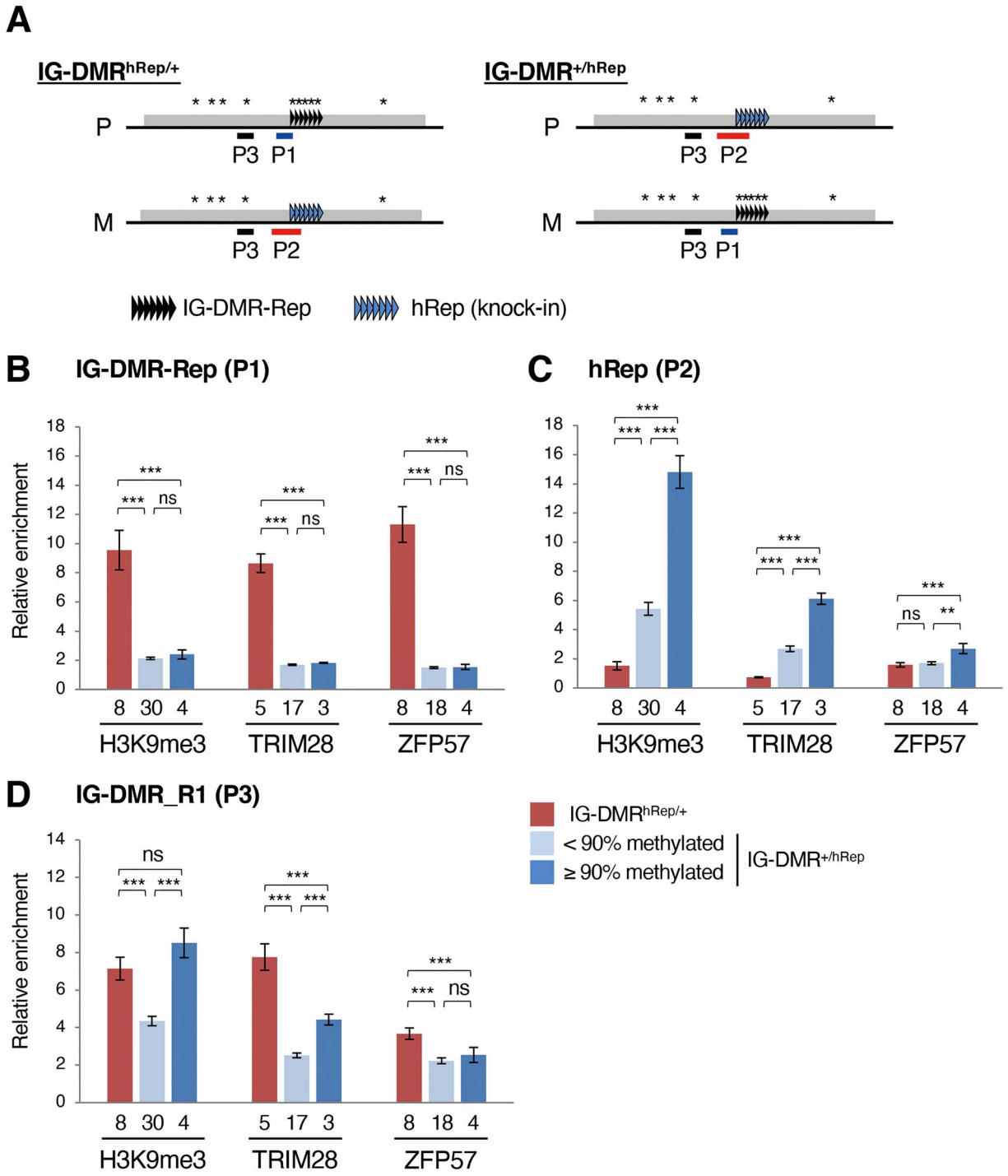

Figure 6. Enrichment of ZFP57–TRIM28 complex in IG-DMR$^{+/hRep}$ embryos. (**A**) Schematic representation of analyzed regions in IG-DMR. Genomic DNA, IG-DMR-Rep and hRep are indicated as for Fig. 2A. Asterisks indicate ZFP57 binding motifs. The PCR-amplified portions for ChIP-qPCR analysis are indicated under the regions. (**B-D**) ChIP-qPCR analysis of IG-DMR-Rep (B), hRep (C) and IG-DMR_R1 (D) in IG-DMR$^{hRep/+}$ (red bar) and IG-DMR$^{+/hRep}$ (light blue bar, <90% methylated at hRep, and dark blue bar, ≥90% methylated at hRep) embryos at 11.5 dpc. Numbers below the graphs indicate sample numbers used for each analysis. The samples were collected from >3 litters. The bar graph represents relative enrichment levels normalized to the enrichment level of the *Gapdh* promoter. Primers used are indicated at the top with parentheses. Antibodies used are shown at the bottom. Error bars indicate standard errors. $^{**}P < 0.01$; $^{***}P < 0.001$; ns: not significant (Student's *t*-test).

hRep sequence does not contain ZFP57-binding motifs, at the beginning of this study, we anticipated that IG-DMR$^{+/hRep}$ mice would exhibit phenotypes similar to those of IG-DMR$^{+/\Delta Rep}$ mice. Indeed, most IG-DMR$^{+/hRep}$ embryos exhibited growth retardation and perinatal lethality due to loss of methylation at the paternal IG-DMR allele, similar to the phenotypes identified in our previous report (15). However, interestingly, a number of IG-DMR$^{+/hRep}$ mice survived and maintained methylation imprint at the hRep sequence. In addition, the diminished fetal weight in IG-DMR$^{+/\Delta Rep}$ embryos by 14.5 dpc was not

observed in any IG-DMR$^{+/hRep}$ embryos. Previously, we reported mice with IG-DMR-Rep replaced by a CpG-free sequence (IG-DMR^{CG-}). These mice inherited the replaced allele paternally (IG-DMR$^{+/CG-}$), and showed reduced fetal weight and placental defects that resulted in embryonic lethality, a similar situation as reported for IG-DMR$^{+/\Delta Rep}$ animals (16). Compared with previous reports, our results suggested that the hRep sequence is able to partially rescue the lethal phenotype caused by IG-DMR-Rep deletion. In addition, our results showed that surviving IG-DMR$^{+/hRep}$ pups had completely methylated paternal hRep, and normally methylated *Meg3*-DMR. IG-DMR$^{+/hRep}$ embryos with such methylation status exhibited monoallelic expression of *Meg3* at normal levels. In contrast, IG-DMR$^{+/hRep}$ pups with hypomethylated *Meg3*-DMR were postnatal lethal, even though paternal hRep was highly methylated. These results suggest that the monoallelic expression of maternally expressed genes by the establishment and maintenance of methylation imprints at *Meg3*-DMR is essential for the survival of IG-DMR$^{+/hRep}$ embryos.

It has been reported that binding of ZFP57 with TRIM28 is an essential mechanism for the maintenance of methylation imprints at IG-DMR (23,24). Methylation imprints at IG-DMR established during spermatogenesis are lost after fertilization and before blastocysts in IG-DMR$^{+/\Delta Rep}$ (Supplementary Material, Fig. S11), suggesting that the methylation imprints of paternal IG-DMR are protected from active/passive demethylation during preimplantation development by maternal and/or zygotic ZFP57 and TRIM28. Consistent with IG-DMR$^{+/\Delta Rep}$ embryos, hRep was completely methylated in sperm, and most hRep lost their methylation imprints during preimplantation development in IG-DMR$^{+/hRep}$. However, some IG-DMR$^{+/hRep}$ individuals maintained hRep methylation. It has been reported that there is a specific dose requirement for TRIM28 at IG-DMR (24). Therefore, this suggests that a sufficient amount of TRIM28 was recruited at paternal hRep in the former group, independent of ZFP57.

Recently, Takahashi *et al.* (25) reported that ZNF445, a KRAB-ZFP, is required for the maintenance of DNA methylation of multiple human imprinted loci, including IG-DMR. Knockdown of ZNF445 in human ES cells results in loss of methylation at human IG-DMR and upregulation of *MEG3*, suggesting that ZNF445 binds to IG-DMR and recruits TRIM28, rather than ZFP57, in humans. However, it is unclear whether ZNF445 binds to the methylated hRep sequence. Mice lacking *Zfp445*, which is an orthologue of the human *ZNF445* gene, displayed no alteration in IG-DMR methylation levels, indicating that ZFP57 predominantly acts as a TRIM28 recruiting factor for IG-DMR in mice (25). Our results showed that ZFP57 binds very weakly, if at all, to hRep in IG-DMR$^{+/hRep}$ embryos. It is not clear whether the presence of endogenous ZFP445 is involved in unstable hRep methylation, but ZFP445, or other KRAB-ZNFs such as ZNF202, is a candidate for an as-yet-unknown factor functioning in place of ZFP57 (26). Further studies are required to understand the molecular mechanisms involving KRAB-ZFP and TRIM28 in the maintenance of methylation imprints at hRep.

Our previous study showed that substitution of IG-DMR-Rep with CpG-free sequence affects other regions in IG-DMR, suggesting that methylation imprints over the entire region of IG-DMR uniformly depend on the methylation level of IG-DMR-Rep. (16) However, interestingly, we found that paternal IG-DMR_R1 was methylated in most IG-DMR$^{+/hRep}$ embryos, whereas a small number of individuals were completely methylated at the paternal IG-DMR_R2 allele. In addition, the monoallelic expression of *Meg3* was observed in IG-DMR$^{+/hRep}$ embryos with methylated paternal IG-DMR_R2, suggesting that embryos with such methylation status would survive. Taken together, these results suggested that methylation of the region containing IG-DMR_R2 is critical for functional imprinting at IG-DMR. There is a distal transcriptional enhancer of *Meg3,* and regions expressing small RNAs near IG-DMR_R2, implying that IG-DMR_R2 methylation might be essential for the regulation of a variety of molecular mechanisms (27,28).

In summary, we identified that the humanization of a tandem repeated sequence stochastically rescued DNA methylation imprints at paternal IG-DMR when IG-DMR-Rep was absent. The mice we generated in this study can provide new insights into regulatory mechanisms involved in IG-DMR-mediated imprinted expression in the human *DLK1-DIO3* domain. In patients with Temple syndrome, epimutation cases involving IG-DMR or *MEG3*-DMR, the causes of which are unknown, have been reported (29). Our results may contribute to an improved understanding of the pathogenesis of these cases.

Materials and Methods

Preparation of sgRNA and donor plasmids

sgRNA, corresponding to 'sg5' in a previous report, was used for microinjection (16). For the construction of the donor plasmid, a human tandem repeat sequence (160 bp, chr14:100810905–100811064/hg38) was PCR amplified from the HEK293T cell line genome, and cloned into the BamHI/HindIII sites of pBlueScriptII-KS(−) vector. Subsequently, homology arms flanking the IG-DMR-Rep were amplified from the C57BL/6 genome, and amplicons were cloned into XbaI/BamHI and HindIII/SalI sites of the vector. Primer sequences are listed in Supplementary Material, Table S1.

Mice

Fertilized eggs were collected from the superovulated F_1 hybrids of C57BL/6 × DBA/2 (BDF1) female mice crossed with BDF1 males (Sankyo Lab Service, Tokyo, Japan). A mixture of 250 ng/μL sgRNA, 100 ng/μL Cas9 protein (Nippon Gene, Toyama, Japan) and 5 ng/μL donor plasmid was injected into the pronuclei and cytoplasm of the zygotes. After overnight culture, embryos that reached the 2-cell stage were transferred into the oviduct of pseudopregnant Jcl:ICR female mice (CLEA Japan, Tokyo, Japan). Founder mice were crossed with C57BL/6 N mice (Sankyo Lab Service), and offspring were crossed with C57BL/6 N or JF1/Ms animals. The JF1/Ms strain was provided by the National Institute of Genetics (Shizuoka, Japan). Genotypes were analyzed by PCR with primers pairs hRep_F/3′ endo_R and 5′ endo_F/hRep_R, as listed in Supplementary Material, Table S1. All animal protocols were approved by the Animal Care and Use Committee of the National Research Institute for Child Health and Development, Tokyo, Japan. All experiments were conducted in accordance with approved animal protocols.

Histological analysis

Placentas at 16.5 dpc were fixed in 4% paraformaldehyde in phosphate buffer saline and then embedded in paraffin. Paraffin sections were stained with hematoxylin and eosin.

Expression analysis of imprinted genes

Total RNA was isolated using ISOGEN (Nippon Gene) and treated with TURBO DNase (Ambion, Austin, TX, USA). cDNA was synthesized using SuperScript II (Thermo Fisher Scientific, Waltham, MA, USA) and oligo dT primer. For expression analysis

of *Rtl1*, cDNA was synthesized using a random primer (Thermo Fisher Scientific). Quantitative RT-qPCR was performed using Power SYBR Green Master Mix (Applied Biosystems, Foster City, CA, USA) and the primers listed in Supplementary Material, Table S1.

Allelic expression analyses were performed by sequencing of PCR products amplified from cDNA using the primers listed in Supplementary Material Table S1.

DNA methylation analysis

DNA was extracted from the tail tips of embryos or pups by phenol/chloroform extraction followed by ethanol precipitation. Two micrograms of DNA was subjected to sodium bisulfite conversion using an EpiTect Bisulfite Kit (QIAGEN, GmbH, Hilden, Germany). For bisulfite sequencing, IG-DMR regions were amplified using EpiTaq HS (Takara Bio, Shiga, Japan) and cloned into pGEM-T Easy (Promega, Madison, WI, USA). Plasmids were amplified with Illustra TempliPhi Amplification Kit (GE Healthcare, Piscataway, NJ, USA) and sequenced.

For DNA methylation analysis of blastocysts, superovulated BDF1 female mice were crossed with IG-DMR^{hRep} males. Embryos at 3.5 dpc were collected by flushing the uteli. Genomic DNA of individual blastocysts was extracted using the alkaline-lysis method. Individual blastocysts were treated with 8 µL of 50 mM NaOH at 95°C for 10 min. Then, 2 µL of 1 M Tris-HCl (pH 8.0) was added. Two microliters of the sample were used for genotyping. The remaining sample was subjected to bisulfite conversion with 2 µg yeast tRNA (Sigma-Aldrich, St. Louis, MO, USA) as a carrier. Nested PCR was carried out using EpiTaq HS with the primers listed in Supplementary Material, Table S1. PCR products were cloned and sequenced as described above.

Methylation levels were analyzed using QUMA (30). DNA methylation data were analyzed only when the bisulfite conversion rate was >95%. Multiple clones were removed by excluding identical bisulfite sequences (included in QUMA).

Chromatin immunoprecipitation

Embryos at 11.5 dpc were divided into tail and body. Tail tissue was used for genotyping and bisulfite analysis. The remaining bodies were homogenized using BioMasher (Nippi, Tokyo, Japan) in PBS containing a proteinase inhibitor cocktail (Sigma-Aldrich). Cross-linked chromatin was sheared using a sonicator (Covaris, Woburn, MA, USA). ChIP experiments were carried out using ChIP Reagent (Nippon Gene) and Dynabeads (Protein A or M-280 anti-mouse IgG, Thermo Fisher Scientific), according to the manufacturer's instructions. DNA was purified using AMPure XP (Beckman Coulter, Brea, CA, USA). Quantitative PCR was performed using Power SYBR Green Mix and the primers listed in Supplementary Material, Table S1.

The following antibodies were used for ChIP: anti-ZFP57 (ab45341; Abcam, Cambridge, UK), anti-TRIM28 (ab10484; Abcam) and anti-H3K9me3 (MABI0308; MBL International, Woburn, MA, USA) (31).

Statistical analysis

At least two biological replicates were performed for all experiments. Statistical differences were determined using Student's *t*-test. For comparison of DNA methylation levels, the Mann–Whitney *U*-test (included in QUMA) was used. $P < 0.05$ was considered statistically significant.

Conflict of Interest Statement

The authors declare that there are no conflicts of interest.

Funding

National Center for Child Health and Development (grant numbers 29–11 and 2020B-1 to S.T.); Young Scientists (B) (grant number 17 K18403 to S.H.); Scientific Research (C) (grant number 19 K06451 to S.H.).

Author Contributions

S.T. designed the experiments. M.T. performed microinjection. A.T.-H. and Y.O. performed genotyping analysis. S.H. carried out almost all molecular experiments. S.H. and S.T. prepared the manuscript.

Acknowledgements

We thank Dr Junko Tomikawa (Kindai University) and Dr Kazuhiko Nakabayashi (National Research Institute for Child Health and Development) for their helpful comments. We also thank all members of the Takada laboratory for technical assistance and animal care. We thank Editage (www.editage.jp) for English language editing.

Supplementary Material

Supplementary Material is available at *HMG* online.

References

1. Tucci, V., Isles, A.R., Kelsey, G., Ferguson-Smith, A.C. and Erice Imprinting Group (2019) Genomic imprinting and physiological processes in mammals. *Cell*, **176**, 952–965.
2. Ferguson-Smith, A.C. (2011) Genomic imprinting: the emergence of an epigenetic paradigm. *Nat. Rev. Genet.*, **12**, 565–575.
3. Moon, Y.S., Smas, C.M., Lee, K., Villena, J.A., Kim, K.H., Yun, E.J. and Sul, H.S. (2002) Mice lacking paternally expressed Pref-1/Dlk1 display growth retardation and accelerated adiposity. *Mol. Cell. Biol.*, **22**, 5585–5592.
4. Sekita, Y., Wagatsuma, H., Nakamura, K., Ono, R., Kagami, M., Hino, T., Suzuki-Migishima, R., Kohda, T., Ogura, A. *et al.* (2008) Role of retrotransposon-derived imprinted gene, *Rtl1*, in the feto-maternal interface of mouse placenta. *Nat. Genet.*, **40**, 243–248.
5. Miyoshi, N., Wagatsuma, H., Wakana, S., Shiroishi, T., Nomura, M., Aisaka, K., Kohda, T., Surani, M.A., Kaneko-Ishino, T. and Ishino, F. (2000) Identification of an imprinted gene, Meg3/Gtl2 and its human homologue MEG3, first mapped on mouse distal chromosome 12 and human chromosome 14q. *Genes Cells*, **5**, 211–220.
6. Hernandez, A., Martinez, M.E., Fiering, S., Galton, V.A. and St Germain, D. (2006) Type 3 deiodinase is critical for the maturation and function of the thyroid axis. *J. Clin. Invest.*, **116**, 476–484.
7. Schmidt, J.V., Matteson, P.G., Jones, B.K., Guan, X.J. and Tilghman, S.M. (2000) The *Dlk1* and *Gtl2* genes are linked and reciprocally imprinted. *Genes Dev.*, **14**, 1997–2002.
8. Seitz, H., Youngson, N., Lin, S.P., Dalbert, S., Paulsen, M., Bachellerie, J.P. and Ferguson-Smith, A.C. (2003) Imprinted microRNA genes transcribed antisense to a reciprocally

imprinted retrotransposon-like gene. *Nat. Genet.*, **34**, 261–262.
9. Hatada, I., Morita, S., Obata, Y., Sotomaru, Y., Shimoda, M. and Kono, T. (2001) Identification of a new imprinted gene, Rian, on mouse chromosome 12 by fluorescent differential display screening. *J. Biochem.*, **130**, 187–190.
10. Takada, S., Tevendale, M., Baker, J., Georgiades, P., Campbell, E., Freeman, T., Johnson, M.H., Paulsen, M. and Ferguson-Smith, A.C. (2000) *Delta-like* and *Gtl2* are reciprocally expressed, differentially methylated linked imprinted genes on mouse chromosome 12. *Curr. Biol.*, **10**, 1135–1138.
11. Kagami, M., Sekita, Y., Nishimura, G., Irie, M., Kato, F., Okada, M., Yamamori, S., Kishimoto, H., Nakayama, M., Tanaka, Y. *et al.* (2008) Deletions and epimutations affecting the human 14q32.2 imprinted region in individuals with paternal and maternal upd(14)-like phenotypes. *Nat. Genet.*, **40**, 237–242.
12. Temple, I.K., Cockwell, A., Hassold, T., Pettay, D. and Jacobs, P. (1991) Maternal uniparental disomy for chromosome 14. *J. Med. Genet.*, **28**, 511–514.
13. Georgiades, P., Watkins, M., Surani, M.A. and Ferguson-Smith, A.C. (2000) Parental origin-specific developmental defects in mice with uniparental disomy for chromosome 12. *Development*, **127**, 4719–4728.
14. Lin, S.P., Youngson, N., Takada, S., Seitz, H., Reik, W., Paulsen, M., Cavaille, J. and Ferguson-Smith, A.C. (2003) Asymmetric regulation of imprinting on the maternal and paternal chromosomes at the *Dlk1–Gtl2* imprinted cluster on mouse chromosome 12. *Nat. Genet.*, **35**, 97–102.
15. Saito, T., Hara, S., Kato, T., Tamano, M., Muramatsu, A., Asahara, H. and Takada, S. (2018) A tandem repeat array in IG-DMR is essential for imprinting of paternal allele at the Dlk1-Dio3 domain during embryonic development. *Hum. Mol. Genet.*, **27**, 3283–3292.
16. Hara, S., Terao, M., Muramatsu, A. and Takada, S. (2019) Efficient production and transmission of CRISPR/Cas9-mediated mutant alleles at the IG-DMR via generation of mosaic mice using a modified 2CC method. *Sci. Rep.*, **9**, 20202.
17. Li, X., Ito, M., Zhou, F., Youngson, N., Zuo, X., Leder, P. and Ferguson-Smith, A.C. (2008) A maternal-zygotic effect gene, Zfp57, maintains both maternal and paternal imprints. *Dev. Cell*, **15**, 547–557.
18. Quenneville, S., Verde, G., Corsinotti, A., Kapopoulou, A., Jakobsson, J., Offner, S., Baglivo, I., Pedone, P.V., Grimaldi, G., Riccio, A. and Trono, D. (2011) In embryonic stem cells, ZFP57/KAP1 recognize a methylated hexanucleotide to affect chromatin and DNA methylation of imprinting control regions. *Mol. Cell*, **44**, 361–372.
19. Messerschmidt, D.M., de Vries, W., Ito, M., Solter, D., Ferguson-Smith, A. and Knowles, B.B. (2012) Trim28 is required for epigenetic stability during mouse oocyte to embryo transition. *Science*, **335**, 1499–1502.
20. Strogantsev, R., Krueger, F., Yamazawa, K., Shi, H., Gould, P., Goldman-Roberts, M., McEwen, K., Sun, B., Pedersen, R. and Ferguson-Smith, A.C. (2015) Allele-specific binding of ZFP57 in the epigenetic regulation of imprinted and non-imprinted monoallelic expression. *Genome Biol.*, **16**, 112.
21. Riso, V., Cammisa, M., Kukreja, H., Anvar, Z., Verde, G., Sparago, A., Acurzio, B., Lad, S., Lonardo, E., Sankar, A. *et al.* (2016) ZFP57 maintains the parent-of-origin-specific expression of the imprinted genes and differentially affects non-imprinted targets in mouse embryonic stem cells. *Nucleic Acids Res.*, **44**, 8165–8178.
22. Paulsen, M., Takada, S., Youngson, N., Benchaib, M., Charlier, C., Segers, K., Georges, M. and Ferguson-Smith, A.C. (2001) Comparative sequence analysis of the imprinted Dlk1-Gtl2 locus in three mammalian species reveals highly conserved genomic elements and refines comparison with the Igf2-H19 region. *Genome Res.*, **11**, 2085–2094.
23. Takahashi, N., Gray, D., Strogantsev, R., Noon, A., Delahaye, C., Skarnes, W.C., Tate, P.H. and Ferguson-Smith, A.C. (2015) ZFP57 and the targeted maintenance of Postfertilization genomic imprints. *Cold Spring Harb. Symp. Quant. Biol.*, **80**, 177–187.
24. Alexander, K.A., Wang, X., Shibata, M., Clark, A.G. and García-García, M.J. (2015) TRIM28 controls genomic imprinting through distinct mechanisms during and after early genome-wide reprogramming. *Cell Rep.*, **13**, 1194–1205.
25. Takahashi, N., Coluccio, A., Thorball, C.W., Planet, E., Shi, H., Offner, S., Turelli, P., Imbeault, M., Ferguson-Smith, A.C. and Trono, D. (2019) ZNF445 is a primary regulator of genomic imprinting. *Genes Dev.*, **33**, 49–54.
26. Monteagudo-Sánchez, A., Hernandez Mora, J.R., Simon, C., Burton, A., Tenorio, J., Lapunzina, P., Clark, S., Esteller, M., Kelsey, G., López-Siguero, J.P. *et al.* (2020) The role of ZFP57 and additional KRAB-zinc finger proteins in the maintenance of human imprinted methylation and multi-locus imprinting disturbances. *Nucleic Acids Res.*, **48**, 11394–11407.
27. Kota, S.K., Llères, D., Bouschet, T., Hirasawa, R., Marchand, A., Begon-Pescia, C., Sanli, I., Arnauld, P., Journot, L., Girardot, M. *et al.* (2014) ICR noncoding RNA expression controls imprinting and DNA replication at the Dlk1-Dio3 domain. *Dev. Cell*, **31**, 19–33.
28. Luo, Z., Lin, C., Woodfin, A.R., Bartom, E.T., Gao, X., Smith, E.R. and Shilatifard, A. (2016) Regulation of the imprinted Dlk1-Dio3 locus by allele-specific enhancer activity. *Genes Dev.*, **30**, 92–101.
29. Kagami, M., Yanagisawa, A., Ota, M., Matsuoka, K., Nakamura, A., Matsubara, K., Nakabayashi, K., Takada, S., Fukami, M. and Ogata, T. (2019) Temple syndrome in a patient with variably methylated CpGs at the primary MEG3/DLK1:IG-DMR and severely hypomethylated CpGs at the secondary MEG3:TSS-DMR. *Clin. Epigenetics*, **11**, 42.
30. Kumaki, Y., Oda, M. and Okano, M. (2008) QUMA: quantification tool for methylation analysis. *Nucleic Acids Res.*, **36**, W170–W175.
31. Kimura, H., Hayashi-Takanaka, Y., Goto, Y., Takizawa, N. and Nozaki, N. (2008) The organization of histone H3 modifications as revealed by a panel of specific monoclonal antibodies. *Cell Struct. Funct.*, **33**, 61–73.